

Characterization and Control of ZnGeN₂ Cation Lattice Ordering

Eric W. Blanton, Keliang He, Jie Shan, Kathleen Kash

Department of Physics, Case Western Reserve University, Cleveland, OH 44106

Abstract

ZnGeN₂ and other heterovalent ternary semiconductors have important potential applications in optoelectronics, but ordering on the cation sublattice, which can affect the band gap, lattice parameters, and phonons, is not yet well understood. Here the effects of growth and processing conditions on the ordering of the ZnGeN₂ cation sublattice were investigated using x-ray diffraction and Raman spectroscopy. Polycrystalline ZnGeN₂ was grown by exposing solid Ge to Zn and NH₃ vapors at temperatures between 758 °C and 914 °C. Crystallites tended to be rod-shaped, with growth rates higher along the c-axis. The degree of ordering, from fully disordered, wurtzite-like x-ray diffraction spectra to orthorhombic, with space group $Pna2_1$, increased with increasing growth temperature, as evidenced by the appearance of superstructure peaks and peak splittings in the diffraction patterns. Annealing disordered, low-temperature-grown ZnGeN₂ at 850 °C resulted in increased cation ordering. Growth of ZnGeN₂ on a liquid Sn-Ge-Zn alloy at 758 °C showed an increase in the tendency for cation ordering at a lower growth temperature, and resulted in hexagonal platelet-shaped crystals. The trends shown here may help to guide understanding of the synthesis and characterization of other heterovalent ternary nitride semiconductors as well as ZnGeN₂.

Keywords: A1. X-ray diffraction, A3. Polycrystalline deposition, B1. Nitrides, B2. Semiconducting materials.

1. Introduction

Heterovalent ternary semiconductors are formed conceptually by replacing the cation or anion sublattice of a wurtzite or zincblende binary semiconductor with an ordered sublattice of two different atom types such that the average number of valence electrons stays the same. These semiconductors often have properties similar to those of their parent binary compounds. For example, in ZnGeN₂ the Ga sublattice of GaN is replaced with equal numbers of Zn and Ge atoms, arranged so that in the lowest enthalpy state each N atom is bound to two Zn and two Ge atoms, and hence the average number of valence electrons remains the same; ZnGeN₂ has a band gap within 100 meV, and lattice spacings within approximately one percent, of those of GaN. However, the

heterovalent ternaries also have interesting and potentially useful differences in comparison to the binaries. Because of the reduced symmetry, heterovalent ternary semiconductors can have high nonlinear optical coefficients [1]. Their more complicated lattices offer more opportunities for doping strategies, and defect and band structure engineering [1]. Furthermore, the degree of ordering on the cation sublattice can be used as a tuning parameter since it can change the optical properties, vibrational properties, and lattice parameters. For example, the band gap of ZnSnP₂ changes by 0.3 eV upon ordering [2]. The greater flexibility of choice in materials provides additional opportunities. For example, ZnSnN₂, composed entirely of abundant elements, might replace InN or Ga_{1-x}In_xN₂ in some applications.

1.1. Cation Sublattice Ordering

The nature of disorder in the heterovalent ternary semiconductors is of both fundamental and practical interest. However, it is not yet well understood. The accepted model is the random placement of atoms on the mixed cation sublattice, which would cause many instances where local charge neutrality is disrupted; the so-called octet rule is thus violated [3]. These defects disrupt the electronic structure of the material, sometimes substantially reducing the band gap. Recent theoretical work on ZnSnN_2 predicts that the band gap disappears altogether when cation disorder consists of many of these octet rule violations. [4]. However, there is an alternative model for disorder on the cation sublattice that does not produce octet rule violations.

In ZnGeN_2 and other wurtzite-based heterovalent ternary semiconductors, there are two ways of ordering the cation lattice that preserve the octet rule. One configuration has the space group $Pna2_1$, shown at the top of Fig. 1. The unit cell has sixteen atoms instead of four as for wurtzite, and the symmetry is orthorhombic [5]. The other way of ordering has the space group $Pmc2_1$ and an eight-atom unit cell, [6], depicted at the bottom of Fig. 1. It has been shown that by randomly stacking $Pna2_1$ - and $Pmc2_1$ -like layers in the crystals y direction, an effectively disordered structure is formed without producing any octet-rule violations [4]. This alternative model of cation disorder could explain why ZnSnN_2 grown by Quayle *et al.* is observed to be disordered, as evidenced by XRD, but also has a band gap that is very close to that of perfectly ordered ZnSnN_2 [4]. Similarly, there are two ways of ordering zincblende-based heterovalent ternary compounds, and a similar model of disorder has been presented for these materials [7, 8].

1.2. Detection of Ordering

The x-ray diffraction (XRD) and Raman spectroscopy measurements used in the present study can differentiate between ordered and disordered material, but not whether the disorder obeys or violates the octet rule.

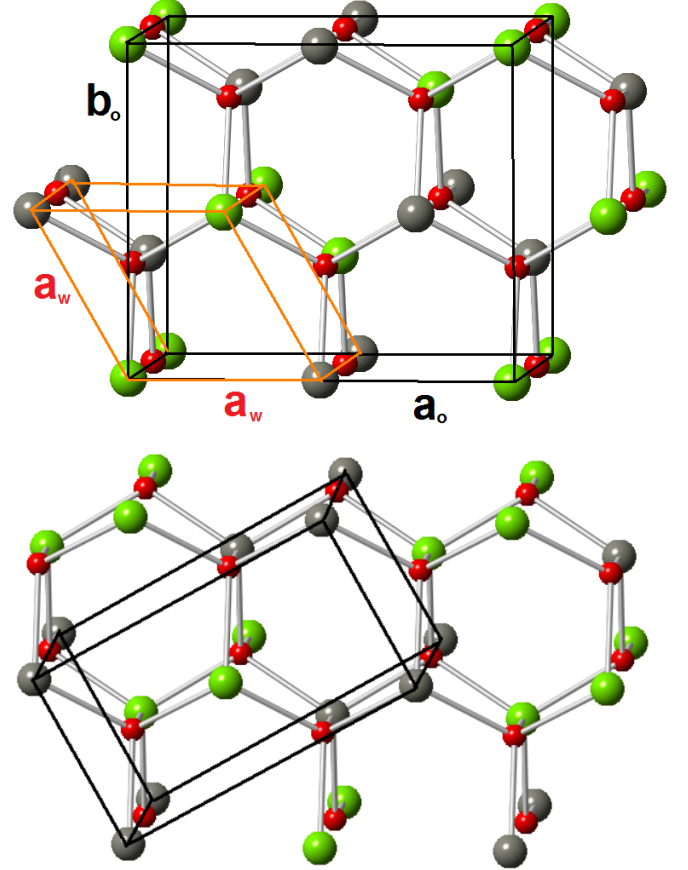


Figure 1: The unit cell of orthorhombic $Pna2_1$ structure (top) and its relation to the wurtzite unit cell. Red spheres are nitrogen, green spheres are germanium, and grey spheres are zinc. Also shown (bottom) is the structure with space group $Pmc2_1$.

Ordering of heterovalent ternary semiconductors is usually detected through XRD. For ternary semiconductors derived from both zincblende and wurtzite lattices, there is often a lattice distortion associated with the cation lattice ordering. In chalcopyrite structures $\frac{c}{a}$ can deviate from the ideal zincblende value of two [9]. In wurtzite-derived orthorhombic structures with space group $Pna2_1$, the a parameter increases and the b parameter decreases, causing $\frac{a}{b}$ to become greater than the ideal wurtzite value of $\frac{2\sqrt{3}}{3}$. These distortions, if large enough, can be detected using XRD through the splitting of many of the peaks.

In the parent binary zincblende and wurtzite structures there are reflections which are extinguished due to the symmetry of the structures. Disordered heterovalent ternary compounds have the same symmetry as their parent binary compounds, so these reflections are still extinguished. An effect of the reduction of symmetry due to ordering is the appearance of superstructure peaks in the XRD pattern from the formerly symmetry-forbidden reflections. The superstructure peaks can be very weak, however, because their presence depends on the difference in scattering cross section between the two cation types. In chalcopyrite, the (101), (217), and (611) peaks are typical superstructure reflections that appear upon ordering [10]. In orthorhombic $Pna2_1$, the (110) and (101) peaks are the strongest superstructure peaks. In $ZnGeN_2$ these superstructure peaks are approximately two orders of magnitude less intense than the strongest peaks, while for $ZnSnN_2$, they are only one order of magnitude less intense [4].

Order-disorder transitions have been observed in many zincblende-based heterovalent ternary semiconductors. At temperatures much lower than the melting temperatures of the compounds, the structure is chalcopyrite. As the temperature is raised, a disorder transition is observed 50-80 °C below the melting point, as evidenced by XRD. For some compounds, the material melts before the order-disorder transition is observed [9].

There has been much less research reported on the wurtzite-based heterovalent ternary compounds. $ZnGeN_2$ and $ZnSiN_2$ [11] have been

grown with ordered $Pna2_1$ lattices. A range of ordering has been observed for $ZnGeN_2$, but until recently it has not been understood how to control the cation lattice ordering [12, 13, 14, 15, 11, 16, 17, 18, 19, 20]. The present study shows that $ZnGeN_2$ grown at lower temperatures tends to have a high degree of disorder on the cation sublattice while at higher temperatures the cation sublattice becomes ordered. In addition, annealing of disordered material at high temperature causes the cation sublattice to order. Recently, Shang et al. reported temperature-dependent ordering in $ZnGeN_2$ produced by annealing Zn_2GeO_4 under NH_3 ; their observations are consistent with the present study [21].

In section 2 of this paper, the experiments probing the control of $ZnGeN_2$ cation lattice ordering are described. In section 3, the XRD and Raman results demonstrating the variation and control of ordering are reported and their implications are discussed.

2. Materials and Methods

$ZnGeN_2$ was grown by reaction of Zn and Ge with gaseous NH_3 in the center of a single-zone quartz tube furnace. In the first set of growths, Zn vapor and NH_3 (Airgas Research Grade) flowed over a [111]-oriented Ge wafer resting on a graphite platform. In GaN growth, the addition of diluent metals such as Na to Ga has been shown to alter the kinetics of the growth. In a slightly modified second set of growths designed to explore the effect of the addition of Sn, a Sn/Ge liquid in equilibrium with a solid Ge wafer was exposed to Zn vapor and NH_3 . For all of the experiments Zn vapor was supplied by evaporating liquid Zn (Alfa Aesar 99.999% purity) from a graphite crucible on the upstream side of the furnace. The Zn partial pressure was controlled by adjusting the crucible position via a bellows-sealed plunger and thereby the crucible temperature. The Ge wafer platform and the Zn crucible temperatures were monitored using type-K thermocouples embedded in the graphite pieces. H_2 from a hydrogen generator (Matheson Chrysalis II) was used as the carrier gas. Gas purifiers (En-

tegris Gatekeeper) were used at the points of injection for the H_2 as well as the high purity N_2 and NH_3 .

2.1. Growths on Ge wafer

Table 1 lists the conditions for a series of four growths on Ge substrates. Prior to being loaded into the chamber, the Ge wafer and Zn were chemically etched to reduce surface oxides. Zn shot (Alfa Aesar 99.999% purity) was melted into a slug, allowed to cool, then was etched in 6:1 $H_2O:HNO_3$ for one minute. The Ge wafer was etched in 10% HF for one minute. To reduce atmospheric O_2 and H_2O contamination in the growth chamber, a series of pump-and-purge operations was performed before each growth. After the Zn and Ge were loaded into the quartz tube, 500 sccm of N_2 was flowed at 0.013 atm for 1 hour, then, the H_2 and NH_3 lines were purged by flowing 120 sccm and 60 sccm of H_2 and NH_3 , respectively, at 0.013 atm for 0.5 hours. To ensure effective purging of the chamber, including stagnant volumes, the pressure was increased to atmospheric pressure with N_2 then evacuated to 0.013 atm. Five of these pump-purge cycles were performed. Subsequently, the furnace was heated to 400 °C while flowing 50 sccm H_2 for approximately 16 hours. This step further reduced atmospheric contamination and accelerated water desorption from chamber walls and reduction of oxides on the Zn and Ge surfaces.

The furnace was then raised to the growth temperature under 60 sccm of H_2 flow at 0.94 atm with the Zn crucible pulled out of the furnace. The temperature was maintained for 0.5 hours to let the temperature gradients at the ends of the furnace equilibrate. The Zn crucible was then pushed into the furnace to the location at which the desired Zn temperature was reached. Once the Zn temperature equilibrated, the NH_3 flow was started in order to initiate $ZnGeN_2$ growth. For all of the experiments, the total flow rate during the growth stage was 60 sccm. The gas flow rates were maintained during the cooling stage.

2.2. Annealing Experiments

For the annealing experiments, disordered $ZnGeN_2$ was grown using the conditions shown in Table 1 for growth 1. After XRD and Raman measurements were performed, the disordered material was loaded back into the chamber for annealing. The pump-purge cycles described in section 2.1 were performed before flowing 100 sccm N_2 at 0.013 atm for approximately 16 hours at room temperature, rather than at the 400 °C temperature used for the growths, in order to avoid decomposition of the $ZnGeN_2$.

At high temperature the rate of decomposition of the $ZnGeN_2$ was found to be sensitive to the ambient gas composition. From separate experiments it was determined that if $ZnGeN_2$ was heated to 850 °C in 0.94 atm of pure N_2 , all of the $ZnGeN_2$ would decompose within one hour, leaving pure Ge on the wafer. Annealing at 850 °C in 0.94 atm of pure NH_3 resulted in complete conversion to Ge_3N_4 in one hour, as evidenced by XRD analysis. Therefore, in order to avoid decomposition of $ZnGeN_2$ during annealing, Zn vapor and NH_3 were flowed while at high temperature, at the partial pressures shown in Table 1. Analysis by optical microscopy before and after annealing under these conditions confirmed that the $ZnGeN_2$ crystals were unchanged in size and shape and that therefore additional $ZnGeN_2$ was not grown during the annealing experiments. As anticipated, the layer of $ZnGeN_2$ already present prevented Ge from reaching the surface to react with the ambient Zn and NH_3 . Table 1 lists the conditions for the two annealing experiments.

2.3. Growths on Ge/Sn Liquid

A modified version of the growth method described in section 2.1 consisted of growing $ZnGeN_2$ on a Ge/Sn liquid. Approximately 0.05 g of Sn (Alfa Aesar 99.999%) was placed on the Ge wafer prior to being loaded into the furnace. Upon heating to the growth temperature of 758 °C, a liquid alloy formed that was in equilibrium with the solid Ge wafer. After the furnace reached the desired temperature, the Zn crucible was pushed into the furnace and heated to the desired temperature. As the Zn partial pressure was increased,

Zn dissolved into the Ge/Sn liquid. The Ge/Sn liquid was left exposed to the Zn pressure for 15 minutes in order for the liquid composition to equilibrate before flowing NH_3 . At the growth conditions, the liquid composition was estimated to be approximately 31% Sn, 15% Zn, and 54% Ge, based on thermodynamic data [22, 23, 24].

2.4. Characterization Methods

Power x-ray diffraction measurements were done with a Bruker Discover D8 with a 2-dimensional detector.

For Raman spectroscopy measurements, either a 633 nm or a 532 nm wavelength laser beam was sent through a 50x objective onto the sample. The beam was defocused so that an area approximately 70 μm wide was illuminated. The scattered light was collected in reflection by the same objective, filtered, and detected by a spectrometer equipped with a liquid-nitrogen-cooled CCD.

3. Results

3.1. Wafer Growths

Fig. 2a and 2b shows SEM micrographs of the surfaces of growths 1 and 3, respectively. Fig. 2c and 2d shows the cross-sections of the cleaved wafers of growth 1 and growth 4, respectively. The smooth area at the bottom of the frame is the underlying Ge wafer. At the higher temperatures a much thicker crust consisting of larger crystals grew, compared to the lower-temperature growths.

Fig. 3 shows the XRD patterns for the four growths. The simulated patterns were made using Crystal Diffract software using lattice parameters derived from the measured patterns, listed in Table 2. The wurtzite simulation was calculated assuming each cation site had an average occupancy of 50% Ge and 50% Zn atoms. The XRD pattern of growth 1, at the lowest growth temperature, is indistinguishable from that of wurtzite, consistent with this material being fully disordered on the cation sublattice. As the growth temperature was increased, the cation ordering increased,

as evidenced by the increased peak splitting observed in the figure. Fig. 3c shows the (210) and (020) peaks with an expanded x-axis. The patterns were fit using Gaussian curves in order to measure the lattice constants and determine approximate phase proportions. It is clear that the peak splitting increased with growth temperature, but the resulting pattern was not always fit well by a single phase. Since there are twice the number of (210) planes as (020) planes in ordered ZnGeN_2 , the (210) peak should be twice the height of the (020) peak. Growth 2 does not have this 2:1 ratio. Instead, the pattern of growth 2 was fit well by a mixture of an ordered orthorhombic phase and a disordered wurtzite phase. In the fit, the orthorhombic phase was constrained to have a 2:1 intensity ratio for the (210) and (020) peaks, and the wurtzite phase was constrained to have the same lattice parameter and peak width as the disordered material of growth 1. Based on the relative peak intensities of the two phases in the fit, growth 2 was determined to be approximately 50% orthorhombic and 50% wurtzite. Growths 3 and 4 were each fit well by the single orthorhombic $Pna2_1$ phase.

Equilibrium thermodynamics predicts that the ordered phase is stable at low temperature and the disordered phase is stable at high temperature. The trend observed here with ZnGeN_2 is opposite to that predicted by thermodynamics, so we conclude that the equilibrium disorder temperature is higher than the temperatures explored here, and the observed disordered samples are in metastable states. We speculate that at the lower growth temperatures, atoms do not have sufficient kinetic energy to overcome barriers to finding the lowest-energy, ordered configuration, while at higher temperatures they do.

The orthorhombic a and b lattice parameters change as the growth temperature is increased, as indicated by the shifting peaks in Fig. 3. The fitted lattice parameters are shown in Table 2. As the growth temperature increases from that of growth 1, 758 $^\circ\text{C}$, increasing fractions of the cation sublattice become ordered. In the beginning stages of ordering we should expect to see some mixing of ordered and disordered material,

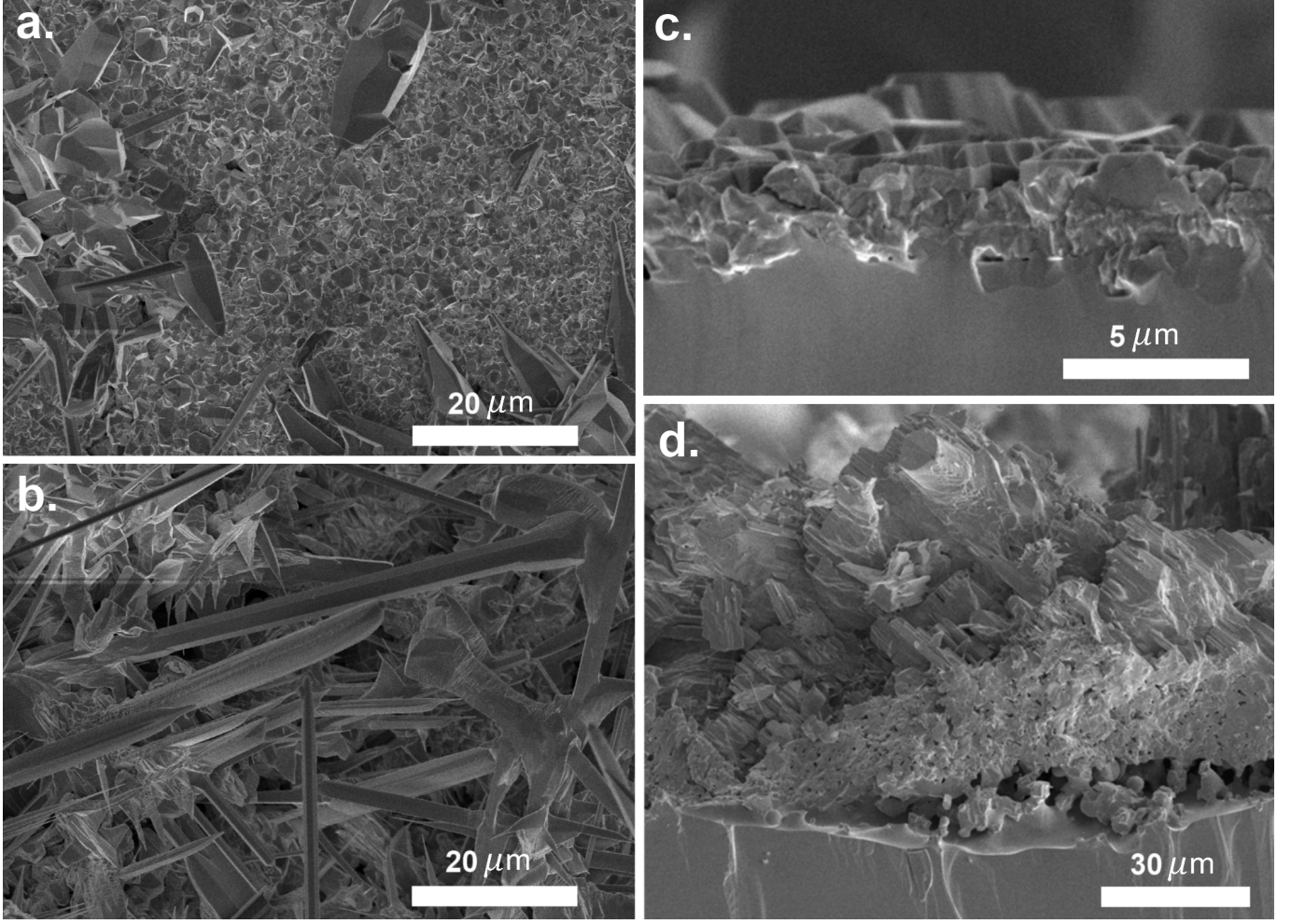


Figure 2: SEM micrographs of wafer growths. a.) surface of growth 1, grown at 758 °C. b.) surface of growth 2, grown at 852 °C. c.) cross section, after cleaving, of growth 1. d.) cross section, after cleaving, of growth 4, grown at 914 °C

which is what we see with growth 2. In these mixtures, regions of ordered ZnGeN_2 are in close proximity to regions of disordered ZnGeN_2 , which has different a and b parameters, so the a and b lattice parameters may not be fully relaxed. As the proportion of ordered material increases, the a and b parameters may be able to more fully relax, resulting in the a parameter growing and the b parameter shrinking with increasing growth temperature. The inhomogeneous strain that may result from the mixing of ordered and disordered material may be the cause here of the broader XRD peaks observed for growths 2 and 3. As shown in Fig. 3c, the deconvolved $Pna2_1$ (210) peak is absent for growth 1, widest for growth 2, then narrows as the material becomes more completely ordered at higher growth temperatures.

Table 2: The fitted lattice parameters. The parameter a was calculated using the (210) and (020) peaks, b using the (020) peak, and c using the (002) peak. The numbers in parentheses are the calculated uncertainties in the last place digits.

Expt.	a (Å)	b (Å)	c (Å)
Growth 1	6.383(5)	5.523(4)	5.192(4)
Growth 2	6.41(1)	5.477(6)	5.189(4)
Growth 3	6.43(1)	5.468(9)	5.190(4)
Growth 4	6.450(4)	5.462(4)	5.193(4)
Anneal 1	6.42(2)	5.486(7)	5.190(4)
Anneal 2	6.43(1)	5.476(6)	5.190(4)
Platelet	6.44(1)	5.468(6)	5.191(4)

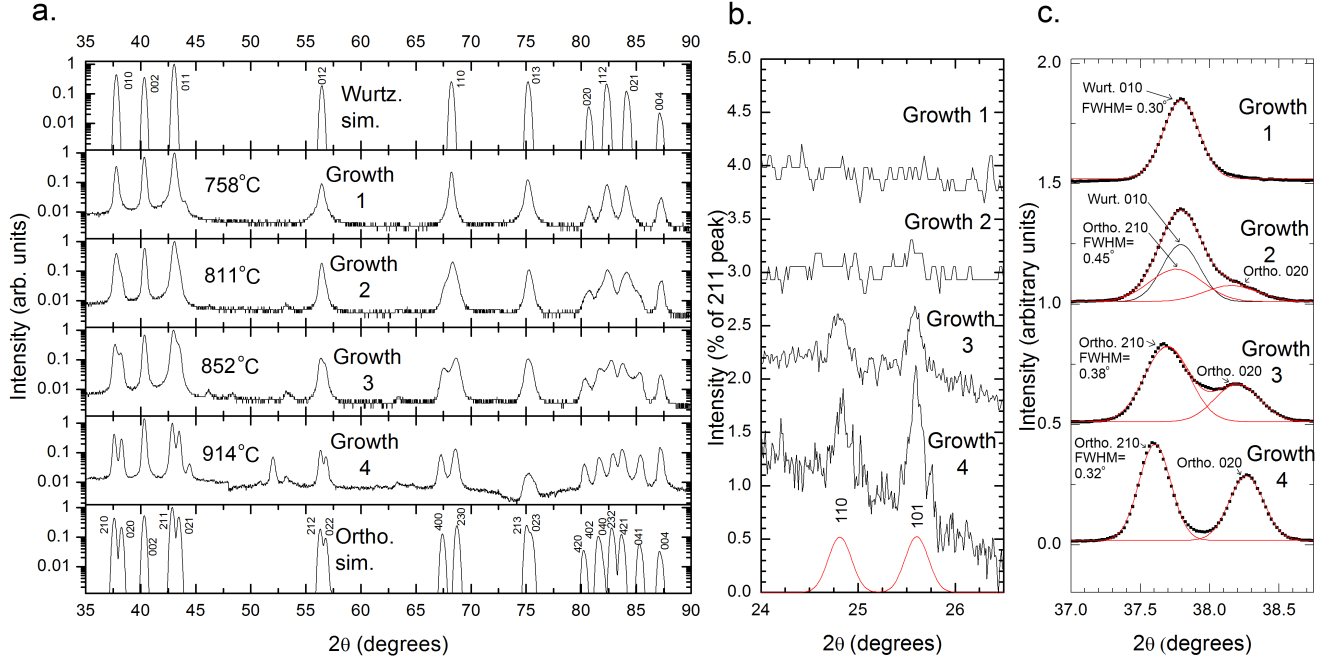


Figure 3: XRD patterns of the four wafer growths. Co K α 1 x-rays were used. a.) The pattern at the top is the simulated wurtzite pattern with each cation lattice site occupied by 50% Ge and 50% Zn density [25]. The pattern at the bottom is the simulated orthorhombic pattern for the space group $Pna2_1$ using the lattice parameters found for wafer growth 4 in Table 2. b.) The portions of the patterns showing the (110) and (101) superstructure peaks. c.) The portions of the patterns showing the (210) and (020) peaks. The fitted width of the (210) peak is listed for each growth.

Table 1: Growth temperatures, gas partial pressures, and durations of the experiments. For all experiments, the total pressure was maintained at 0.94 atm and the total flow rate was maintained at 60 sccm.

Expt.	Growth Temp. ($^{\circ}\text{C}$)	P_{Zn} (atm)	P_{NH_3} (atm)	P_{H_2} (atm)	P_{N_2} (atm)	Duration (hours)
Growth 1	758	0.027	0.31	0.63	0	3.7
Growth 2	811	0.056	0.24	0.70	0	4.0
Growth 3	852	0.028	0.31	0.63	0	1.5
Growth 4	914	0.028	0.47	0.47	0	2.0
Anneal 1	850	0.03	0.47	0	0.47	1.0
Anneal 2	850	0.03	0.47	0	0.47	4.0
Platelet	758	0.03	0.31	0.63	0	4.0

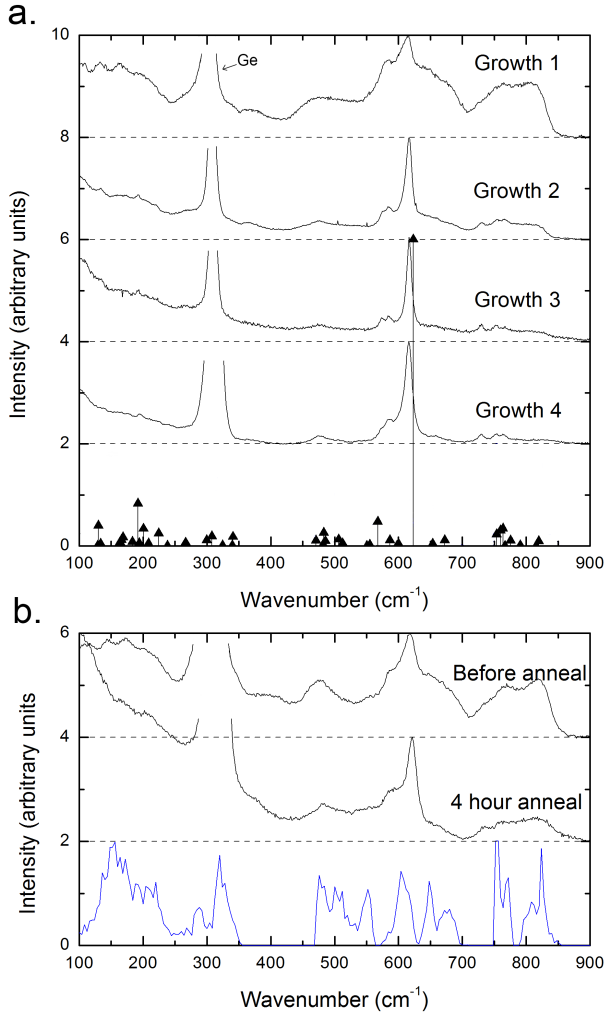


Figure 4: Raman spectra for polycrystalline ZnGeN_2 a) for the four wafer growths and b) after annealing the disordered material for four hours. The triangles at the bottom of a) are all of the calculated Raman active modes in ZnGeN_2 [26]. In b), the blue curve is the calculated phonon density of states [26].

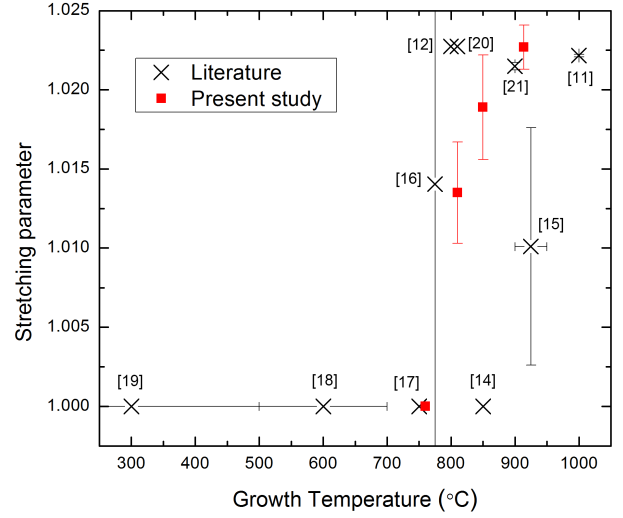


Figure 5: The relation between cation lattice ordering and growth temperature for the ZnGeN_2 reported here and for ten reported growths in the literature. The stretching parameter $\alpha = \frac{3a}{2b\sqrt{3}}$ is a measure of the orthorhombic lattice distortion and is used here as a measure of the extent of ordering. The references from which the data were taken are shown in brackets.

Here we compare the lattice parameters of ZnGeN_2 in the literature to our results, as functions of growth temperature. We introduce the stretching parameter, $\alpha = \frac{3a}{2b\sqrt{3}}$, where a and b are the orthorhombic lattice parameters, to quantify the orthorhombic cation lattice ordering. A wurtzite structure viewed in the orthorhombic unit cell has an $\frac{a}{b}$ ratio of $\frac{2\sqrt{3}}{3}$, so disordered material has α equal to 1, and partially or fully ordered material has α greater than 1. Fig. 5 plots the stretching parameter α for the four wafer growths in the present study and for ten ZnGeN_2 growths reported in the literature, as a function of growth temperature. All of the ZnGeN_2 lattice parameters reported in the literature were converted to the orthorhombic system for ease of comparison. Below growth temperatures of approximately 760 °C, all reported material is disordered (wurtzite). Above this temperature, almost all material is reported to have some amount of orthorhombic ordering.

Fig. 3b shows, for the material reported here, the portion of the XRD pattern containing the

(110) and (101) superstructure peaks. The pattern for growth 1 shows no superstructure peaks, consistent with that material being completely disordered. The pattern of growth 2 shows small peaks consistent with partial ordering. The patterns of growths 3 and 4 show (110) and (101) peak heights consistent with the prediction for fully ordered $Pna2_1$ material, using atomic positions from [5]. To our knowledge measurement of these superstructure peaks for $ZnGeN_2$ using XRD has not been reported by any other group to date.

Disorder on the cation lattice disrupts the phonon modes of ordered $ZnGeN_2$, and therefore Raman spectroscopy can be used as an additional method to probe the disorder. The micro-Raman spectra for the four growths are shown in Fig. 4. The spectra are normalized so that the large peak at 616 cm^{-1} in each spectrum has the same intensity relative to the background above 850 cm^{-1} . As the growth temperature is decreased, the sharpness of the observed peaks decreases and the phonon DOS features increase. As the disorder increases, the momentum conservation rules are relaxed and phonons from across the Brillouin zone participate in the scattering. In a previous study on single crystal $ZnGeN_2$, strong DOS features were observed in the Raman spectra [27]. The trend toward greater ordering with higher growth temperature observed here in the Raman spectra is consistent with that observed in the XRD patterns.

3.2. Annealing Experiments

Data from two annealing experiments are shown here. Disordered $ZnGeN_2$ samples were annealed at $850\text{ }^\circ\text{C}$ for either one or four hours in the presence of Zn and NH_3 vapor. Fig. 6 shows the (210) and (020) XRD peaks for the material before and after the annealing experiments. The first pattern is fit well by wurtzite, consistent with the material being fully disordered. Peak splitting is evident after one hour of annealing and increases after four hours, consistent with the material becoming increasingly ordered with longer annealing time. The peaks were fit with Gaussian curves to find the lattice parameters and propor-

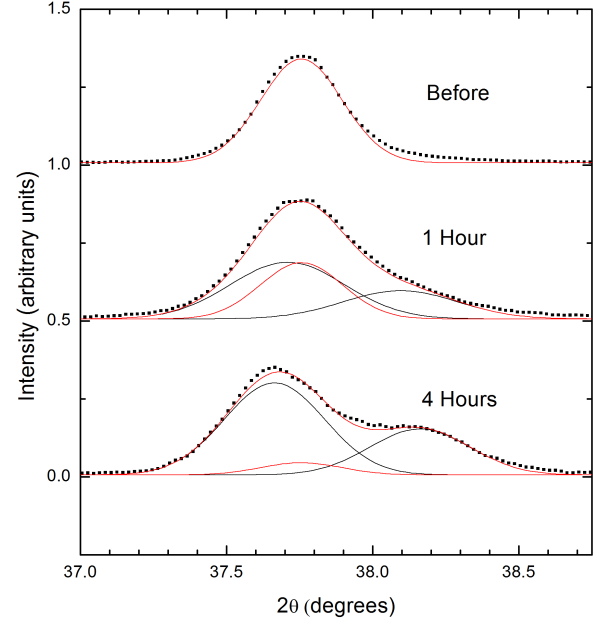


Figure 6: Portion of the XRD pattern showing the (210) and (020) peaks for disordered as-grown $ZnGeN_2$ and after one or four hours of annealing at $850\text{ }^\circ\text{C}$.

tions of the phases present, as for the analysis described in section 3.1. After one hour of annealing, the material was approximately 60% ordered, and after four hours, approximately 90% ordered.

Fig. 4b shows the micro-Raman spectra for the disordered material and after four hours of annealing. The trend is similar to that of the four wafer growths in Fig. 4a.

3.3. Platelets

Both the ordering and morphology of $ZnGeN_2$ were affected substantially when Sn was added to the Ge wafer. Without Sn, the growth rate along the c axis was more than an order of magnitude larger than along the a and b axes, and hexagonally faceted rod-shaped structures resulted. When Sn was added the growth rate along the a and b axes was one to two orders of magnitude higher than along the c axis, resulting in platelet-like structures. Fig. 7 a. shows a SEM micrograph of the $ZnGeN_2$ platelets. The specific reasons for the change in morphology with the addition of Sn are not understood at this time.

In addition to $ZnGeN_2$, some trace amounts of ZnO grew as evidenced in the XRD pattern. ZnO

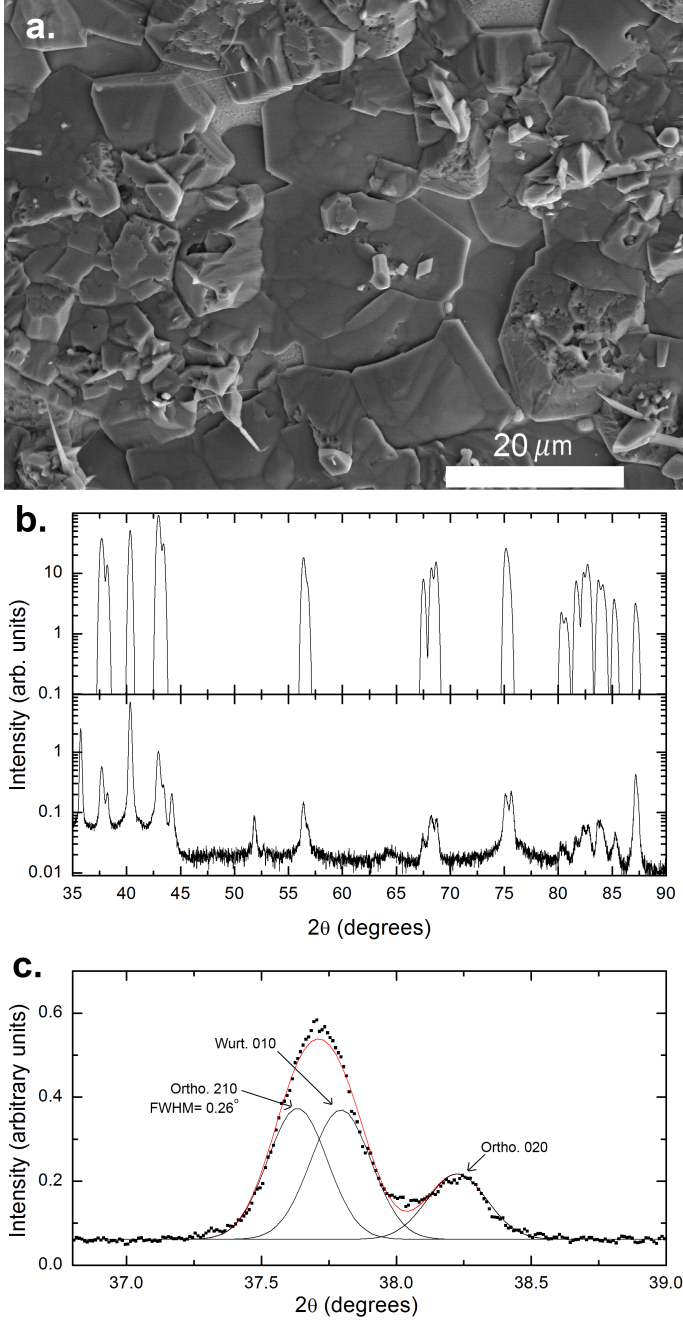


Figure 7: a.) SEM micrograph of ZnGeN₂ platelets grown on a Ge-Sn-Zn liquid. b.) measured XRD pattern of the platelets and a simulated pattern of a mixture of 66% ordered orthorhombic ZnGeN₂ and 34% disordered wurtzite ZnGeN₂. c.) portion of the XRD pattern showing the (210) and (020) peaks. The (210) peak width is shown.

was not present in any of the growths done without Sn present. We hypothesize that the presence of Sn catalyzes the growth of ZnO from remaining impurities. The ZnO was removed by etching the sample in a 2.5% HCl:water solution for six minutes. The XRD pattern shown in Fig. 7 was taken after the ZnO was removed.

Growing on the Sn liquid resulted in cation lattice ordering at a lower growth temperature when compared with the growths on Ge wafers. Fig. 7b shows the XRD pattern of the platelets, grown at 758 °C, which is the same temperature as growth 1 on a Ge wafer in section 3.1. The platelets are almost completely ordered, as evidenced by the XRD pattern, while the material grown at the same temperature on a Ge wafer is completely disordered. The specific reasons for the change in ordering are not understood at this time but might be related to the change in preferential growth direction.

Analysis of the XRD pattern of this growth revealed that the ZnGeN₂ was approximately 66% ordered orthorhombic and 34% disordered (wurtzite). The XRD pattern of the ZnGeN₂ grown in the presence of Sn liquid has narrower peaks than that of the partially ordered material grown without Sn. For example, the orthorhombic (210) peak for the former is approximately 0.3° FWHM, while that for the latter is approximately 0.4° FWHM. This observation leads to the speculation that for the material grown in the presence of Sn the crystal lattices are more relaxed, which suggests that the ordered and disordered phases may exist in separate crystallites. For the material grown without Sn, the two phases may be mixed within single crystallites and thus the lattices are less relaxed.

Since ZnGeN₂ and ZnSnN₂ can in principle be alloyed together, we must consider the possibility that the material grown in the presence of Sn is a ZnGeN₂-ZnSnN₂ alloy. Comparing the *c* parameter of the platelets in Table 2 with the other growths reveals that they are equal within the uncertainty of the measurements. Using Vegards law, the uncertainty in the *c* parameter of ± 0.004 Å is equivalent to a ZnSnN₂ volume fraction of $0 \pm 1.5\%$.

4. Conclusions

These synthesis experiments showed that it is possible to control the cation lattice ordering of ZnGeN_2 by varying the growth temperature and by annealing. The material was disordered at the lowest temperature growth (758 °C) and became progressively more ordered as the growth temperature was increased to 914 °C. The equilibrium disorder transition temperature is most likely significantly higher than the temperatures explored here, and so the disordered samples observed here are most likely in metastable states. Growth or annealing at higher temperatures resulted in material closer to the equilibrium ordered $\text{pna}2_1$ state. Ordering was detected and quantified using the peak splitting and appearance of superstructure peaks in the measured XRD patterns. The trend between disorder and increase of phonon DOS features in Raman spectra was consistent with the trend observed with the XRD patterns.

Growth on a Sn-based liquid decreased the temperature at which ordered ZnGeN_2 was produced. This modified growth method also changed the crystal morphology, resulting in hexagonal platelets instead of hexagonally faceted rod-shaped crystals.

5. Acknowledgements

E.B. and K.K. were supported by the National Science Foundation grants DMR-1006132 and DMR-1409346. J.S. and K.H. acknowledge support from the National Science Foundation grant DMR-1106225.

References

References

- [1] W. R. L. Lambrecht, A. Punya, Heterovalent ternary II-IV-N₂ compounds: perspectives for a new class of wide-band-gap nitrides, in: B. Gill (Ed.), III-Nitride Semiconductors and their Modern Devices, Oxford University Press, 2013, pp. 519–585. doi:10.1093/acprof:oso/9780199681723.001.0001.
- [2] P. St-Jean, G. Seryogin, S. Francoeur, Band gap of sphalerite and chalcopyrite phases of epitaxial zn-snp_2 , Applied Physics Letters 96 (23) (2010) 231913.
- [3] M. Buerger, The temperature-structure-composition behavior of certain crystals, Proc. Natl. Acad. Sci. 20 (1934) 444.
- [4] P. C. Quayle, E. W. Blanton, A. Punya, G. T. Junno, K. He, L. Han, H. Zhao, J. Shan, W. R. L. Lambrecht, K. Kash, Charge-neutral disorder and polytypes in heterovalent wurtzite-based ternary semiconductors: The importance of the octet rule, Phys. Rev. B 91 (2015) 205207. doi:10.1103/PhysRevB.91.205207. URL <http://link.aps.org/doi/10.1103/PhysRevB.91.205207>
- [5] A. Punya, W. R. L. Lambrecht, M. van Schilfgaarde, Quasiparticle band structure of zn-iv-n_2 compounds, Phys. Rev. B 84 (2011) 165204. doi:10.1103/PhysRevB.84.165204. URL <http://link.aps.org/doi/10.1103/PhysRevB.84.165204>
- [6] L. Lahourcade, N. C. Coronel, K. T. Delaney, S. K. Shukla, N. A. Spaldin, H. A. Atwater, Structural and optoelectronic characterization of rf sputtered zn-snn_2 , Advanced Materials 25 (18) (2013) 2562–2566.
- [7] S.-H. Wei, L. . G. Ferreira, A. Zunger, First-principles calculation of the order-disorder transition in chalcopyrite semiconductors, Physical Review B 45 (5) (1992) 2533.
- [8] S.-H. Wei, S. Zhang, A. Zunger, Band structure and stability of zinc-blende-based semiconductor polytypes, Physical Review B 59 (4) (1999) R2478.
- [9] L. Garbato, F. Ledda, A. Rucci, Structural distortions and polymorphic behaviour in $\text{abc } 2$ and $\text{ab } 2 \text{ c } 4$ tetrahedral compounds, Progress in crystal growth and characterization 15 (1) (1987) 1–41.
- [10] S. Francoeur, G. Seryogin, S. Nikishin, H. Temkin, X-ray diffraction study of chalcopyrite ordering in epitaxial $\text{zn-snp} \{ \text{sub } 2 \}$ grown on gaas , Applied physics letters 74 (24).
- [11] T. Endo, Y. Sato, H. Takizawa, M. Shimada, High-pressure synthesis of new compounds, $\text{zn-sin } 2$ and $\text{zn-gen } 2$ with distorted wurtzite structure, Journal of materials science letters 11 (7) (1992) 424–426.
- [12] M. Maunaye, J. Lang, Préparation et Propriétés de ZnGeN_2 , Mater. Res. Bull 5 (1970) 793.
- [13] M. Wintenberger, M. Maunaye, Y. Laurent, Groupe spatial et ordre des atomes de zinc et de germanium dans ZnGeN_2 , Mat. Res. Bull. 8 (1973) 1049.
- [14] W. L. Larson, H. P. Maruska, A. Stevenson, Synthesis and Properties of ZnGeN_2 , J. Electrochem. Soc. 121 (1974) 1683.
- [15] K. Du, C. Bekele, C. C. Hayman, J. C. Angus, P. Pirouz, K. Kash, Synthesis and Characterization of ZnGeN_2 grown from Elemental Zn and Ge Sources, J. Cryst. Growth 310 (2008) 1057.
- [16] T. Misaki, A. Wakahara, H. Okada, A. Yoshia, Epitaxial growth and characterization of ZnGeN_2 by metalorganic vapor phase epitaxy, J. Cryst. Growth 260 (2004) 1049.

- [17] T. J. Peshek, Studies in the growth and properties of ZnGeN_2 and the thermochemistry of GaN , Ph.D. thesis, Case Western Reserve University (2008).
- [18] L. Zhu, P. Maruska, P. Norris, P. Yip, L. Bouthillette, Epitaxial Growth and Structural Characterization of Single Crystalline ZnGeN_2 , MRS Internet J. Nitride Semicond. Res. 4S1 (1999) G3.8.
- [19] S. Kikkawa, H. Morisaka, Rf-sputter deposition of Zn-Ge nitride thin films, Solid state communications 112 (9) (1999) 513–515.
- [20] R. Viennois, T. Taliercio, V. Potin, A. Errebbahi, B. Gil, S. Charar, A. Haidoux, J.-C. Tédénac, Prospective investigations of orthorhombic ZnGeN_2 : synthesis, lattice dynamics and optical properties, Mater. Sci. Eng. B 82 (2001) 45–49.
- [21] M. Shang, J. Wang, J. Fan, H. Lian, Y. Zhang, J. Lin, ZnGeN_2 and ZnGeN_2 : Mn^{2+} phosphors: hydrothermal-ammonolysis synthesis, structure and luminescence properties, Journal of Materials Chemistry C 3 (36) (2015) 9306–9317.
- [22] B.-J. Lee, Thermodynamic assessments of the Sn-Zn and In-Zn binary systems, Calphad 20 (4) (1996) 471–480.
- [23] Z. Long, F. Yin, Y. Liu, J. Wang, H. Liu, Z. Jin, Thermodynamic description of the $\text{Ru}(\text{Si, Ge})\text{-Sn}$ ternary systems, Journal of phase equilibria and diffusion 33 (2) (2012) 97–105.
- [24] R. Olesinski, G. Abbaschian, The Ge-Zn (germanium-zinc) system, Journal of Phase Equilibria 6 (6) (1985) 540–543.
- [25] [link].
URL <http://www.crystallmaker.com/crystalldiffract/>
- [26] T. R. Paudel, W. R. L. Lambrecht, First-principles study of phonons and related ground-state properties and spectra in Zn-IV-N_2 compounds, Phys. Rev. B 78 (11) (2008) 115204. doi:10.1103/PhysRevB.78.115204.
URL <http://link.aps.org/abstract/PRB/v78/e115204>
- [27] T. J. Peshek, T. R. Paudel, K. Kash, W. R. L. Lambrecht, Vibrational modes in ZnGeN_2 : Raman study and theory, Phys. Rev. B 77 (23) (2008) 235213. doi:10.1103/PhysRevB.77.235213.
URL <http://link.aps.org/abstract/PRB/v77/e235213>